

Richard F. Niedziela, Daniel Olesak, Juan Cuecha and Brandon Roman

Department of Chemistry and Biochemistry, College of Science and Health, DePaul University, 1110 West Belden Avenue, Chicago, IL 60614

Introduction

It is widely recognized that organic aerosols constitute a large portion of the overall concentration of particulate matter in the atmosphere. Difficulties remain, however, in our ability to quantify their impact on areas ranging from air quality to human health, particularly those particles that are a result of anthropogenic activity.¹ Perhaps one of the largest sources of organic material in urban atmospheres are gasoline and diesel engines.² Along with exhaust gases, these engines can directly emit organic particles or contribute other materials that result in the secondary formation of aerosols. The mixture of fuel and lubricants, both subject to the intense heat and pressure of the combustion process, serve as source materials for these particles.³ Diesel engines, for example, are known to produce nanoparticles that may pose health risks due to their size and concentration.⁴

Several studies aimed at characterizing engine-related particles have been reported in the literature. For example, Miracolo, *et al.* performed chamber experiments to study the photo-oxidation formation of secondary aerosols from diesel exhaust.⁵ Weitkamp, *et al.* examined the stability of petroleum biomarkers against oxidation by OH to assess the ability to use them to relate aerosol concentrations to vehicle emissions.⁶ Finally, Guzman-Morales, *et al.* used a number of different methods to investigate the amount of primary and secondary aerosol formation in California, including the use of mid-infrared Fourier Transform Infrared (FTIR) spectroscopy.⁷

For some time now, our laboratory has been involved in characterizing the mid-infrared optical properties of pure organic materials by measuring their frequency-dependent complex refractive indices, $N = n + ik$, where n , the real component, governs the ability of the material to scatter light and k , the imaginary component, is related to photon absorption. These data, when coupled with an appropriate optical model, may be used to predict how a sample of matter absorbs and scatters light. Conversely, complex refractive indices may also be used to obtain basic physical information from any given sample of matter. For example, quantities such as particle size, shape and composition may be obtained from a careful analysis of an aerosol extinction spectrum using a suitable retrieval method.⁸

In this presentation, we report on the retrieval of mid-infrared complex refractive indices for two commercially available motor oils. These data may be used is a number of different analytical settings including remote sensing applications and particle size analyses.

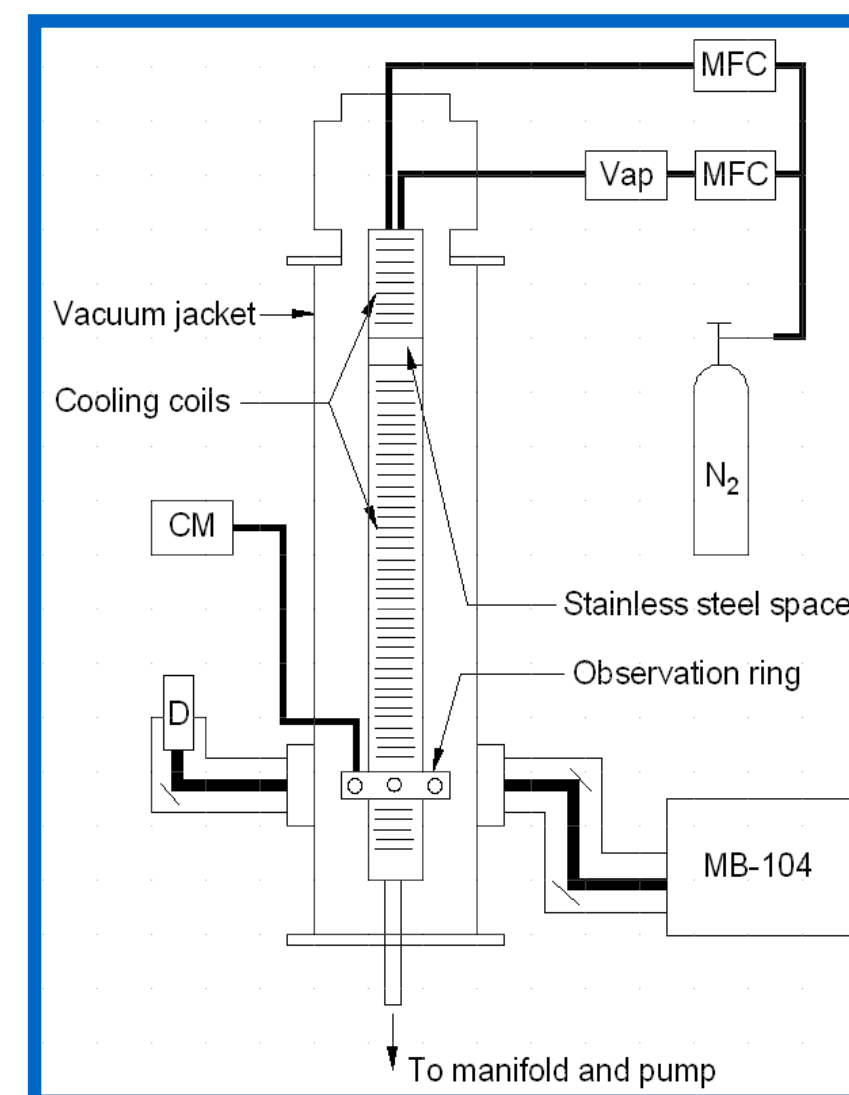
Experimental

All aerosols were homogenously generated by a glass vaporizer described previously.⁸ Pennzoil 0W-20 and 5W-20 samples were used in the vaporizer without further purification. The aerosols were admitted into a glass mixing bulb (Figure 1) where they were diluted before being injected into the vertical aerosol flow cell. MKS 1179A mass flow controllers regulated the flows of dry nitrogen through the vaporizer and mixing bulb at cell pressures ranging from 100 torr to 700 torr at a temperature of 25 °C. Aerosol extinction spectra, were recorded with an ABB Bomem MB-104 FTIR (128 co-additions) operating at a resolution of 2 cm⁻¹ over the range from 750 cm⁻¹ to 5000 cm⁻¹ using a liquid nitrogen cooled HgCdTe detector.



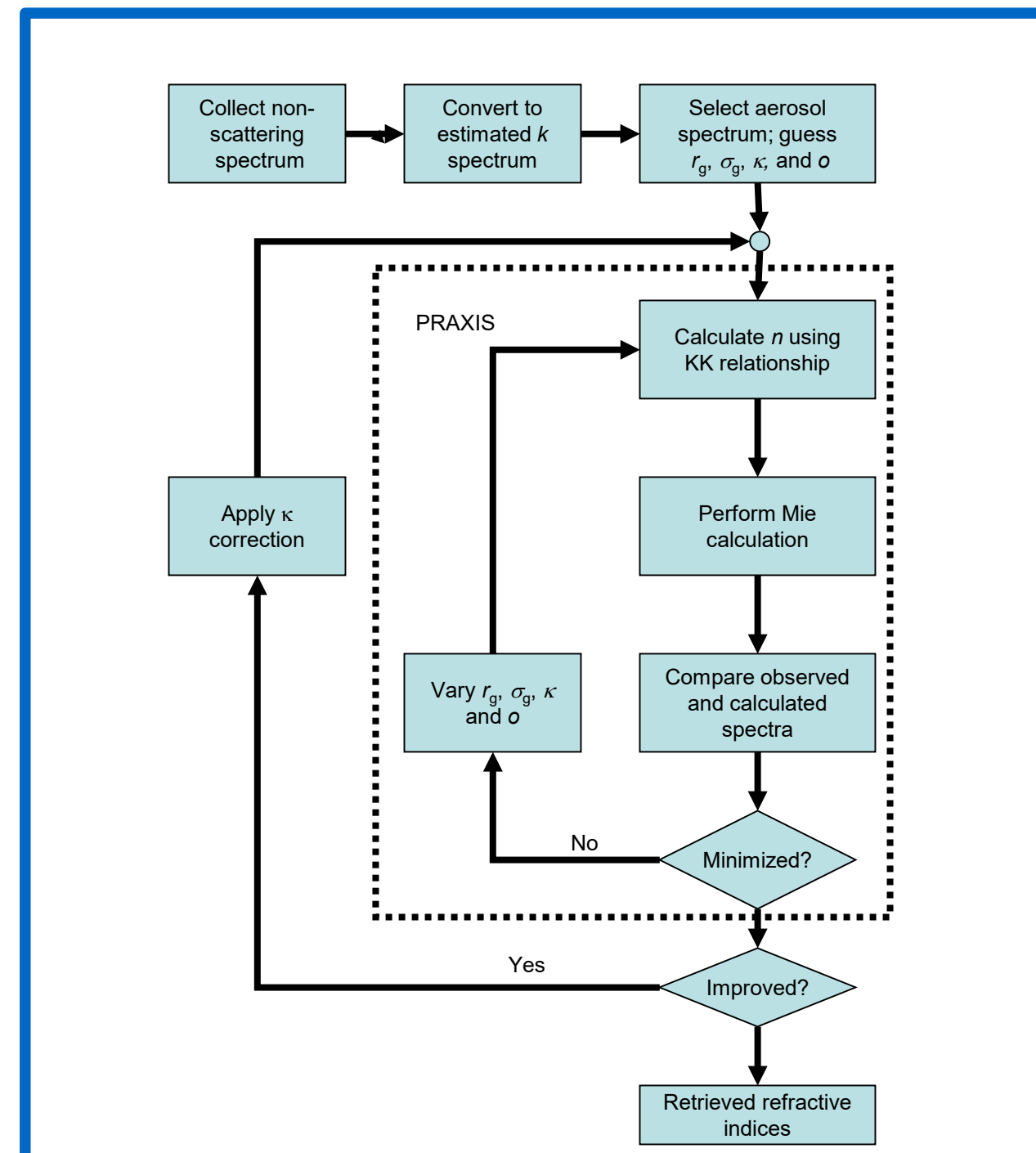
Figure 1: (Left) Photograph of the glass vaporizer and the glass mixing bulb. Aerosols are injected into the flow cell through the bottom of the bulb.

Figure 2: (Right) Schematic of aerosol flow cell system used to record particle extinction spectra in this study. Note that mixing bulb is not shown in this drawing.



Retrieval

Refractive indices were retrieved directly from aerosol extinction spectra using the iterative non-linear procedure described by Dohm *et al.*⁸ with a baseline parameter that compensates for detector drift. A flowchart of the retrieval procedure is shown to the right.



Results and Discussion

The retrieval process requires two key data: a non-scattering spectrum of the material under study which provides an estimate of the imaginary index as a function of wavenumber and its real refractive index at the sodium D-line (589.0 nm). Thin-film spectra taken on a salt plate with a ABB Bomem DA3.02 spectrometer provide the former while temperature-dependent indices were recorded with a Reichert Arias 500 Abbé refractometer for the latter. Figure 3 and 4 show these results, respectively.

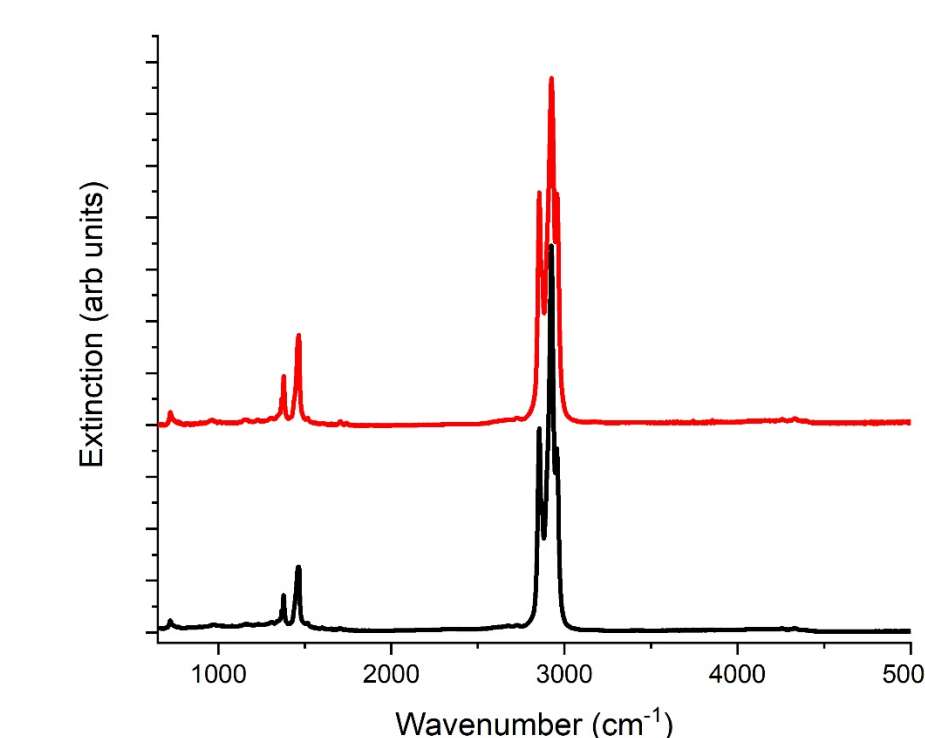


Figure 3: Thin-film spectra used to initiate the retrieval procedure. The 0W-20 sample is shown in red, while the 5W-20 one squalene is in black. The samples generally share the same band locations, however, there are some minor differences in relative intensity in the band structure.

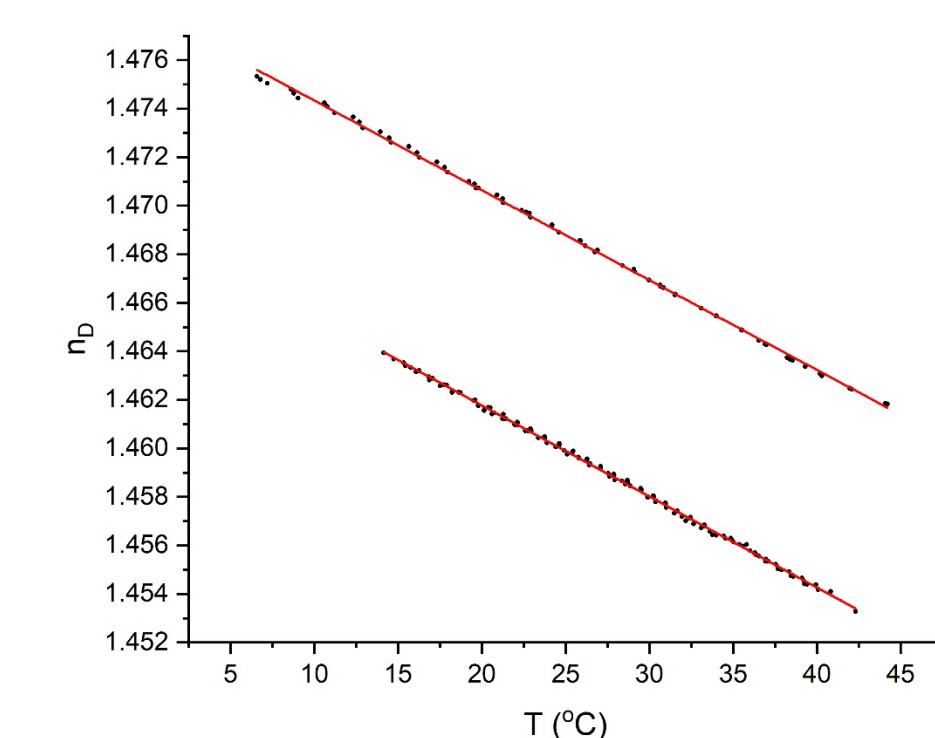


Figure 4: Temperature-dependent real indices for 0W-20 (lower set) and 5W-20 (upper set). Linear fits to these data yield values of 1.45990 ± 0.00004 and 1.46879 ± 0.00005 , respectively, at 25 °C. These values are required to compute the real components via the Kramers-Kronig transform used in the retrieval procedure.

The retrieval process also requires a large collection of aerosol extinction spectra that show signs of scattering which is indicated by curvature in the baseline. Figure 5 shows an example of two such spectra for the 0W-20 sample. The extent of scattering is controlled by the temperature of the vaporizer (250 °C to 450 °C) and the flow of nitrogen through it (0.1 to 1.0 standard liters per minute).

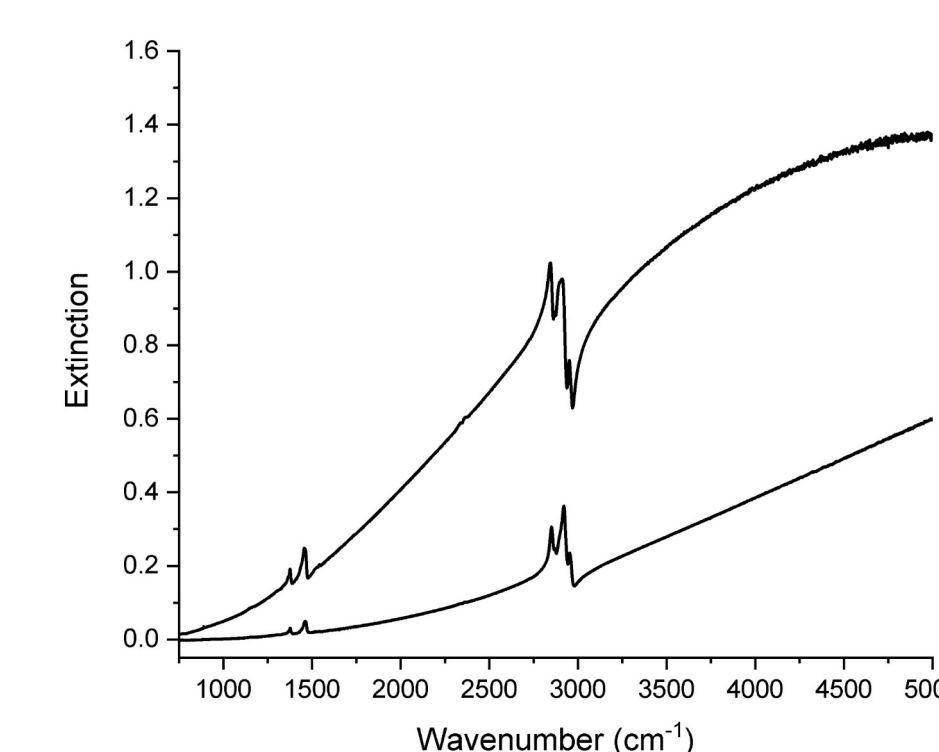


Figure 5: Two scattering aerosol extinction spectra for particles made from 0W-20 motor oil. The curvature in the baseline is due to scattering of light by the aerosol ensemble. The relative amounts of scattering and absorption in these spectra allow the retrieval process to converge to unique solutions.

Figures 6 and 7 show the imaginary and real components, respectively, for the 0W-20 and 5W-20 motor oil samples. Components for squalene (C₃₀H₆₂), a long chain alkane, are included for comparison. Figure 6 features band structures near 3000 cm⁻¹ and just below 1500 cm⁻¹, all of which are consistent with alkane vibrational modes.

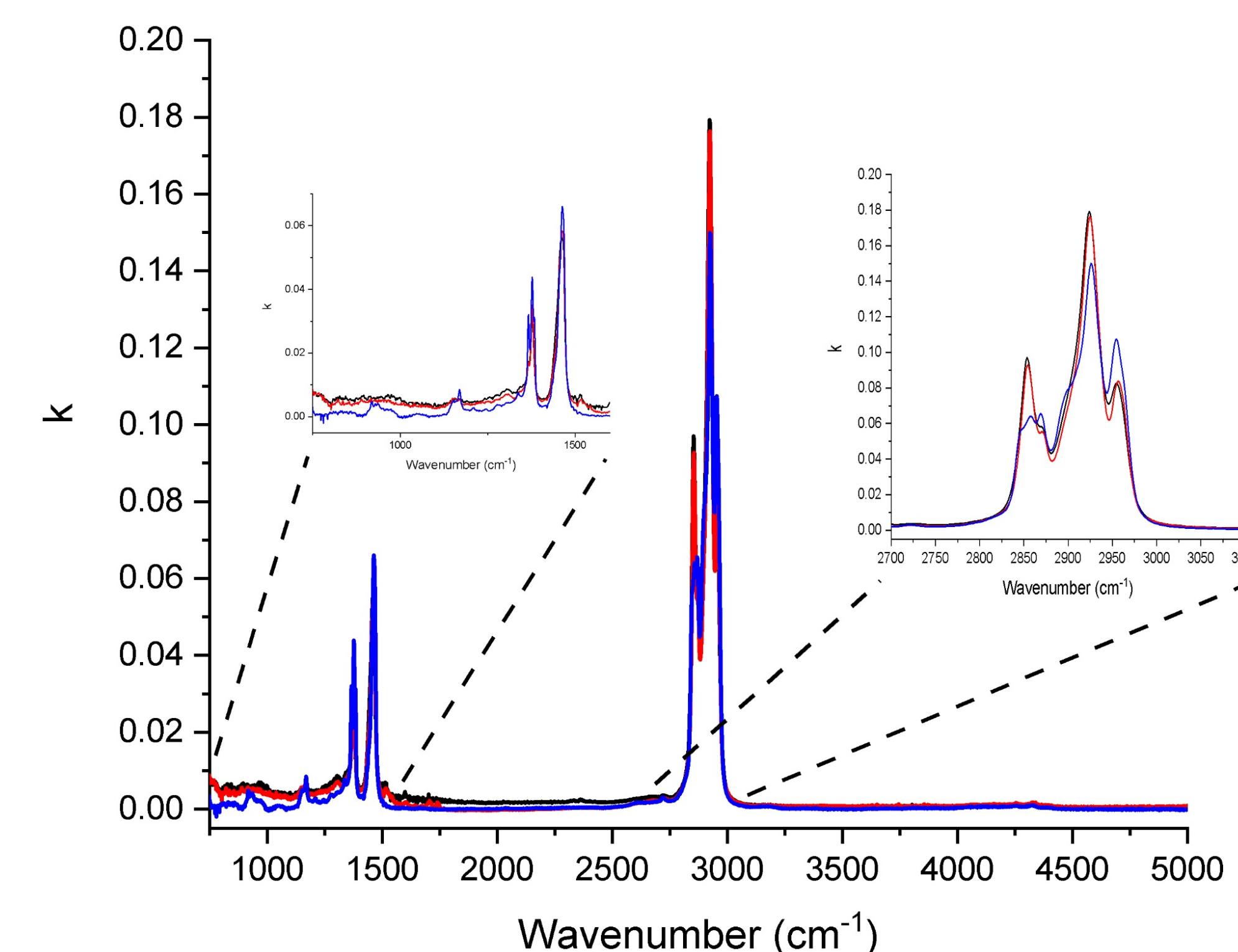


Figure 6: Imaginary components for 0W-20 (red), 5W-20 (black), and squalene (blue) at 25 °C. Bands at 2954, 2923, 2869, and 2855 cm⁻¹ are common alkane markers in fuel standards.⁷

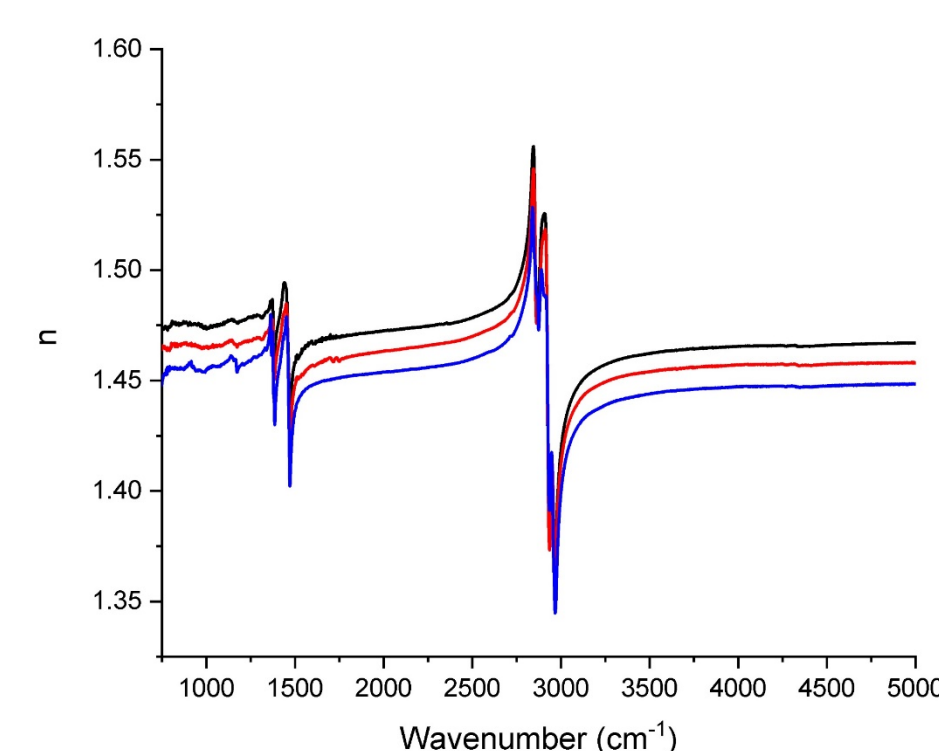


Figure 7: Real refractive index components for 0W-20, 5W-20 and squalene between 750 cm⁻¹ and 5000 cm⁻¹.

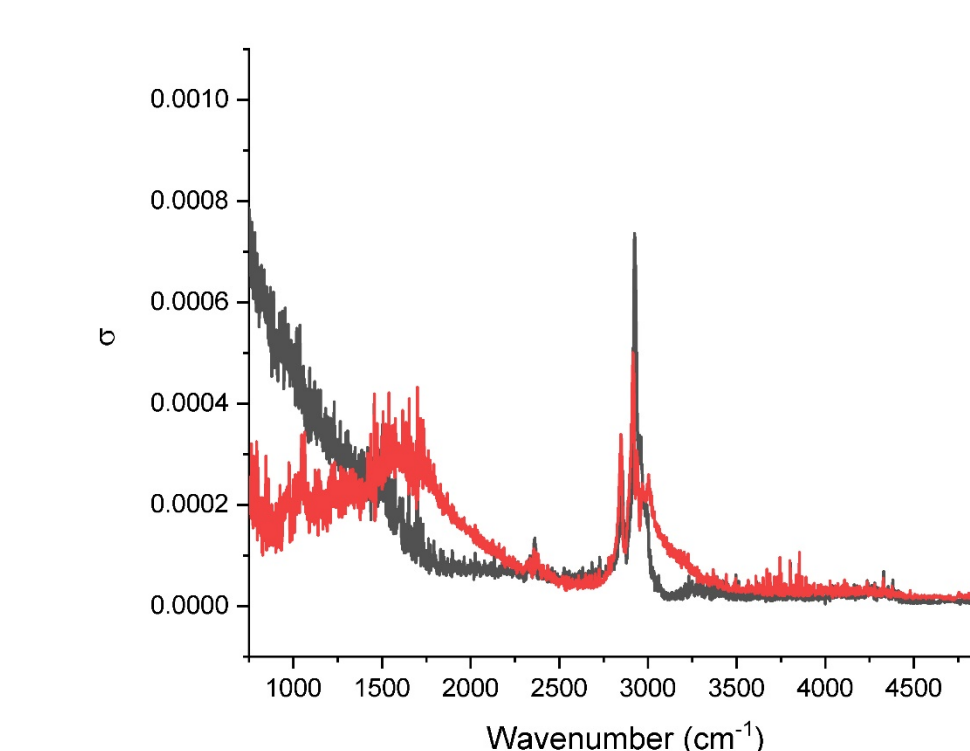


Figure 8: Uncertainties in k (black) and n (red) components for 5W-20 motor oil as determined from 30 retrievals.

Figure 9 shows the application of complex refractive indices in retrieving aerosol properties. The 5W-20 data set was used in a Mie fit of an aerosol extinction spectrum that was not used in the index retrieval. The fit yielded a log-normal size distribution characterized by radius 0.63 μm and a width of 1.54. A Mie fit of the same extinction spectrum was done using the squalene refractive index data set. The fit yielded a radius of 0.65 μm and a width of 1.54, however, there are deviations in the structure of the bands.

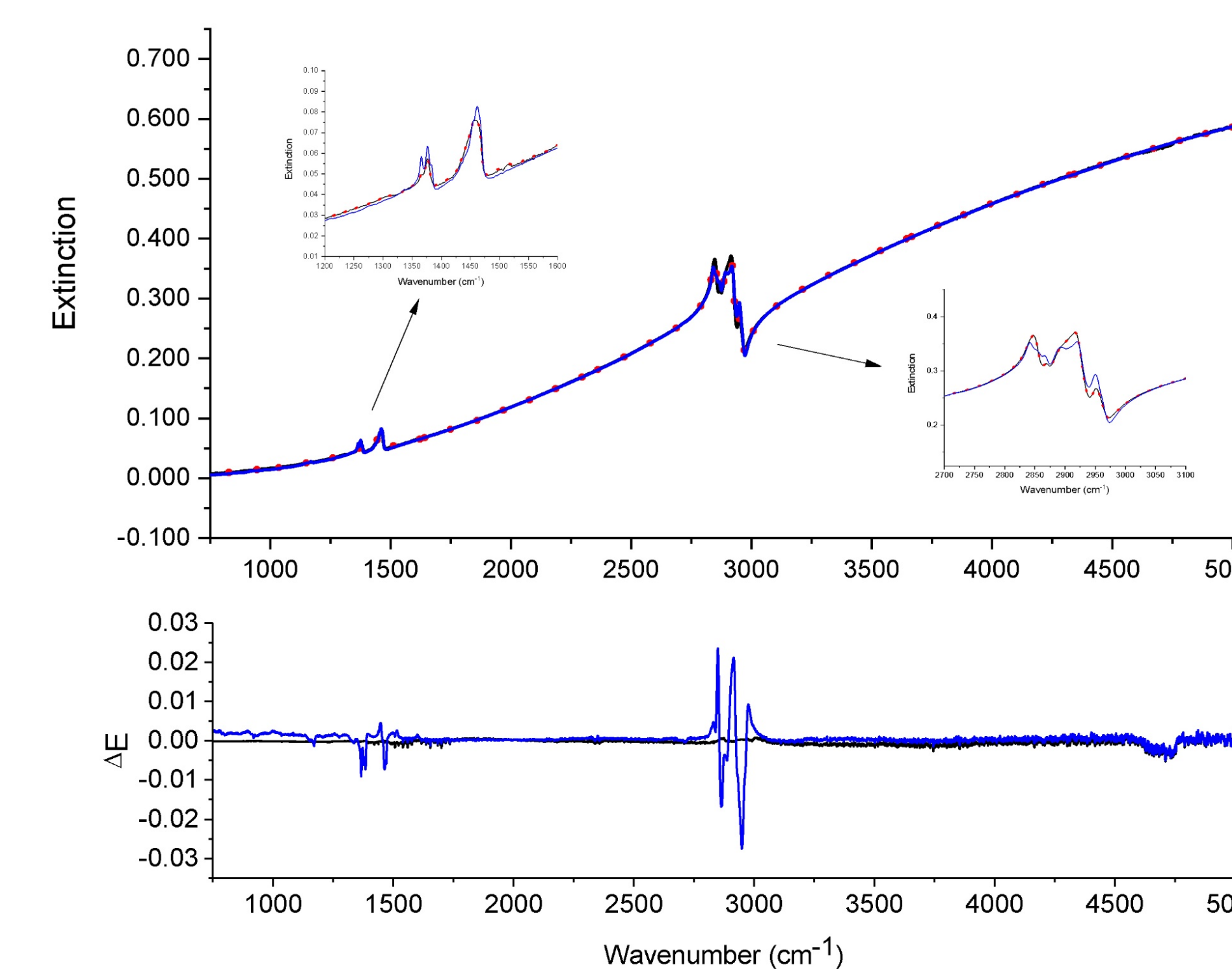


Figure 9: The top panel shows a Mie fit (red dots) of a 5W-20 aerosol extinction spectrum (black). Also shown is a Mie fit of the same spectrum using squalene refractive indices. Both fits yield the same log-normal size distribution parameters, however, there are deviations in the band structure. The lower panel shows the fit deviations for the 5W-20 indices (black) and the squalene indices (blue).

Conclusion

The complex refractive indices reported here are the first known ones for two commercially available 0W-20 and 5W-20 motor oils. The indices are structurally similar to one another and share many of the same features as squalene, a long-chain alkane previously studied in our laboratory. The indices may be used in a variety of aerosol-related applications including particle sizing (see Figure 9). Indeed, the squalene indices were successfully used as a proxy to determine the log-normal particle size parameters for a 5W-20 aerosol. In addition to fresh motor oil samples, we intend to investigate the optical properties of used motor oils.

References

1. B.J. Turpin, P. Saxena and E. Andrews, *Atmos. Environ.*, **34**, 2983-3013, 2000.
2. J.J. Schauer, W.F. Rogge, L.M. Hildemann, M.A. Mazurek, G.R. Cass and R.T. Simoneit, *Atmos. Environ.*, **30**, 3837-3855, 1996.
3. B. Giechaskiel, M. Maricq, L. Ntziachristos, C. Dardiotis, X. Wang, H. Axmann, A. Bergmann and W. Schindler, *J. Aerosol Sci.*, **67**, 48-86, 2014.
4. H. Sakurai, H.J. Tobias, K. Park, D. Zarling, K.S. Docherty, D.B. Kittelson, P.H. McMurry and P.J. Ziemann, *Atmos. Environ.*, **37**, 1199-1210, 2003.
5. M.A. Miracolo, A.A. Presto, A.T. Lambe, C.J. Hennigan, N.M. Donahue, J.H. Kroll, D.R. Worsnop and A.L. Robinson, *Env. Sci. Technol.*, **46**, 1638-1643, 2010.
6. E.A. Weitkamp, A.T. Lambe, N.M. Donahue and A.L. Robinson, *Env. Sci. Technol.*, **42**, 7950-7956, 2008.
7. J. Guzman-Morales, A.A. Frossard, A.L. Corrigan, L.M. Russell, S. Liu, S. Takahama, J.W. Taylor, J. Allan, H. Coe, Y. Zhao and A.H. Goldstein, *Atmos. Environ.*, **88**, 330-340, 2014.
8. M.T. Dohm, A.M. Potscavage and R.F. Niedziela, *J. Phys Chem A*, **108**, 5365-5376, 2004.
9. C.D. Keefe and J.L. MacDonald, *J. Molec. Liq.*, **105**, 121, 2005.
10. A. Tuntuno, C.L. Tien and S.H. Park, *Combust Sci Tech*, **84**, 133, 1992.